

Tetrahedral structures and phase transitions in III-V semiconductors

J. Crain, R.O. Piltz, G. J. Ackland, and S. J. Clark

Department of Physics and Astronomy The University of Edinburgh, Mayfield Road, Edinburgh, Scotland EH9 3JZ, United Kingdom

M. C. Payne, V. Milman, and J. S. Lin

Cavendish Laboratory, University of Cambridge, Madingley Road, Cambridge CB3 0BE, United Kingdom

P. D. Hatton and Y. H. Nam

Department of Physics and Astronomy The University of Edinburgh, Mayfield Road, Edinburgh, Scotland EH9 3JZ, United Kingdom

(Received 16 March 1994; revised manuscript received 10 May 1994)

The BC8 structure (body-centered cubic with eight atoms per cell) is a known pressure-induced modification of both silicon and germanium. However, its diatomic analogue [the SC16 structure (a simple cubic lattice with a basis of 16 atoms)] has never been found in compound semiconductors. We find from total-energy pseudopotential calculations that the SC16 structure is a stable high-pressure polymorph of the III-V semiconductors GaAs, InAs, and AlSb. We report *ab initio* calculations of the structural, electronic, and vibrational properties of SC16-GaAs. The wurtzite structure is found to be unstable at all pressures for each compound considered. We consider possible transition routes consistent with our high-pressure x-ray diffraction results and propose that the formation of the SC16 structure in compounds is kinetically inhibited by the formation of wrong bonds at the structural transition.

I. INTRODUCTION

In recent years there has been considerable renewed interest in the high-pressure properties of semiconductors. This has partly been due to advances in high-pressure x-ray crystallography such as the development and implementation of the image-plate (IP) area detector for angle-dispersive powder diffraction. The enhanced sensitivity afforded by IP technology¹ has allowed the observation of very subtle pressure-induced effects such as the formation of defects at structural transitions and the observation of short-lived metastable phases. These observations have recently been the subject of several *ab initio* calculations which have served to place the interpretation of the experimental data on a firm theoretical foundation.²

Despite these experimental and theoretical advances, very little information is available regarding the nature of the mechanism associated with these highly reconstructive first-order transitions. From an experimental point of view, the problem is a very difficult one. These pressure-induced structural transitions do not preserve single crystals and therefore powder diffraction is the only viable technique for detailed structural studies. Unfortunately, orientational information is lost in a powder diffraction experiment and transition paths cannot be determined unambiguously.³ Even sophisticated first-principles molecular dynamics methods are not appropriate for this problem because of the relatively long time scales over which these transitions occur. Thus information regarding transition routes must be obtained via more indirect methods. For example, some insight into the mechanism of structural phase transitions in tetrahe-

dral semiconductors has been provided by light scattering experiments which revealed that diamond and zinc-blende semiconductors exhibit pressure-induced softening of the lowest acoustic (TA) zone boundary phonons⁴ suggestive of possible lattice instabilities.

Upon increase of pressure, both the group-IV elemental and III-V compound semiconductors display broadly similar behavior in which the diamond or zinc-blende phase transforms to a sixfold coordinated metallic structure having a crystal structure similar to that of either β -Sn or NaCl. It is now well established that depressurization of silicon and germanium from their respective metallic modifications results in dense metastable crystalline phases characterized by fourfold coordination but with distortions from ideal tetrahedral bonding.^{5,6} Previous results^{7,8} have suggested that, in carbon, distortion of the tetrahedral bonding can be extremely unfavorable. It has been suggested that this is connected with the orthogonalization of the closely bound $2p$ electrons as opposed to the $3p$ shell: this explanation would not apply in any of the compounds studied here, so it is interesting to see whether a different mechanism accounts for their apparent instability. These dense phases of group-IV elements have recently been the subject of an extensive first-principles investigation in which it was found that the metastability of these phases could be understood on the basis of total-energy considerations derived from density functional calculations.^{7,9} In this paper we consider the related question of whether, by the same methods, it is possible to explain why these structures are not observed in the compound semiconductors.

The paper is organized as follows. Details of the BC8 and SC16 structures are presented in the next sec-

tion. Then structural studies on recovered (depressurized) phases of compound semiconductors are described with a view to understanding the nature and completeness of the reverse transition. We then describe the techniques used in the *ab initio* total-energy and finite temperature molecular dynamics calculations. Results of these calculations (including total energy differences for relaxed structures, electronic structure, and vibrational properties) are then presented and finally possible transition paths between the sixfold coordinated metallic phase and either BC8 or SC16 phases are considered.

II. STRUCTURAL DETAILS

Silicon adopts a body-centered-cubic structure (called BC8) with eight atoms per primitive cell upon depressurization from the metallic β -Sn phase. Depressurized germanium transforms from the β -Sn structure to a simple tetragonal structure called ST12, which contains 12 atoms per unit cell. The BC8 structure has also recently been observed to exist for short periods in Ge if depressurization is sufficiently rapid.¹⁰

The crystal structure of BC8-Si (Si-III) has been described in detail elsewhere,^{5,6} but we give some essential details below. At ambient pressure, the lattice constant of BC8-Si is $a_0 = 6.64 \text{ \AA}$ and the crystallographic space group is $Ia\bar{3} (T_h^7)$. All the sites of the BC8 structure are equivalent. There is a single free positional parameter x , which has been determined by x-ray diffraction to be approximately 0.1003.⁶ The silicon BC8 structure is comprised of distorted tetrahedrally coordinated ions arranged such that the density is approximately 10% greater than diamond. This increase in density is achieved without large deviations from ideal Si-Si bond lengths, but with substantial angular distortions and consequent reduction of symmetry.

Every atom in the BC8 structure of Si has associated with it one A bond and three longer B bonds. The lengths of these bonds at ambient pressure are $R_A = 2.30 \text{ \AA}$ and $R_B = 2.39 \text{ \AA}$,⁶ respectively. A center of inversion exists at the midpoint of the A bond. The normal bond length of diamond structure silicon is 2.35 \AA . The single nearest nonbonded neighbor is at a distance (R_5) of approximately 3.443 \AA away. This distance is significantly shorter than the next-near-neighbor distance of 3.84 \AA in diamond structure silicon.

The metastability of BC8-Si with respect to diamond-Si, can be qualitatively understood in terms of the topological differences between the two structures. In particular, a BC8 to diamond structural transition which proceeds via shear distortion would require breaking and subsequent rebonding of approximately one-quarter of all tetrahedral bonds and would clearly involve a very high energy barrier to transition. As pointed out by Biswas *et al.*,¹¹ fewer broken bonds are required to transform BC8 to the hexagonal diamond or lonsdaleite structure to which BC8-Si transforms upon annealing. The possibility of forming III-V compound analogues of the lonsdaleite structure will be considered in a later section. Since the BC8 structure is characterized by even-membered rings

(the smallest of which is sixfold), it is possible to construct a diatomic analogue of the BC8 structure in which only unlike species are bonded. However, the eight atom primitive unit cell which is appropriate for homopolar solids cannot be constructed without introducing like-species bonds for diatomic compounds. If the BC8 structure is considered as a simple cubic lattice with a basis of 16 atoms, then two types of atoms can be arranged without like-species bonds. The resulting structure is called SC16. A projection of the diatomic SC16 structure is shown in Fig. 1.

The SC16 structure has lower symmetry (cubic, $P2_13$) than BC8, in particular it is not centrosymmetric. The effect of this is that the structure is described fully by two internal parameters, which can most easily be regarded as one x_i for each species i . The atom neighbor separations depend on the lattice constant and internal parameter through the relations

$$R_A = a_0\sqrt{3}(x_1 + x_2), \quad (1)$$

$$R_B = a_0\sqrt{2(x_1 + x_2)^2 - (x_1 + x_2) + 0.25}, \quad (2)$$

$$R_5 = \sqrt{3}a_0(0.5 - 2x_1), \quad \sqrt{3}a_0(0.5 - 2x_2), \quad (3)$$

where the numerical suffixes on the x 's label atomic species and are relevant only for the SC16 compound. Surprisingly, the lengths of the covalent bonds in SC16 depend only on one parameter, the average of these two x 's. The distances to the nearest nonbonded neighbor (R_5) are now species dependent, requiring the appropriate x value to be used in Eq. (3).

If it were possible to form the SC16 structure in the III-V compounds, an increase in either of the positional parameters x_i would give the piezoelectric strain corresponding to the major axis of the polarizability tensor. In addition, the SC16 structure with its distorted tetrahedral units provides a tractable "complex crystal model" of amorphous heteropolar semiconductors having short-

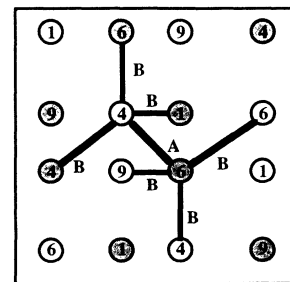


FIG. 1. Projection of the diatomic equivalent of the BC8 structure (SC16 structure) with $x_1 = x_2 = 0.1$. A cubic unit cell containing 16 atoms is shown and the bonds of the central tetrahedral unit are illustrated as black lines. No like-species bonds are present. Elevations in fractional units of $c/10$ are indicated by the numbers inside the circles. Different species are denoted by different shading.

range disorder and zero like-species bonds. Studies of the electronic structure and optical properties of GaAs in the SC16 structure have been made using the empirical pseudopotential method in an effort to simulate some of the essential structural features of amorphous GaAs.¹² While the BC8 structure has not been reported except in silicon and germanium, it has been noted that it has some similarity to the distorted tetrahedral structures known to exist in antimonides of zinc and cadmium.^{6,13}

The metastable phase formed in germanium by gradual depressurization (ST12) is significantly more complex than BC8. It has no obvious diatomic analogue because its odd-membered rings would require bonding between atoms of the same species. Estimates for the wrong-bond energy in zinc-blende GaAs and InSb have been made by consideration of inversion domain boundary defects. The results of these calculations suggest that the wrong bond energy is between 0.2 and 0.5 eV per wrong bond,¹⁴ suggesting that ST12 compounds will be unlikely to form as a result of its inherent defects. As a result, for the remainder of the paper, we will consider only the prospect of forming the SC16 structure and/or the diatomic equivalent of lonsdaleite in compound semiconductors.

III. EXPERIMENTAL STUDIES ON RECOVERED PHASES OF COMPOUND SEMICONDUCTORS

A. Experimental method

We have investigated a range of III-V semiconductors using the IP method^{1,15} with a view to exploring the nature of the recovered phase formed by depressurization from the metallic modification. Powdered samples were loaded into a diamond-anvil pressure cell (Mao and Bell design) along with a methanol-ethanol (4:1) mixture and a ruby pressure calibrant. The pressure was increased in steps from ambient until the metallization transition was reached and then decreased in steps back to ambient. X-ray diffraction measurements were performed both on the upstroke and downstroke steps in pressure. The measurements were performed on Station 9.1 of the Daresbury Laboratory Synchrotron Radiation Source (SRS). The incident x-ray beam was collimated to a size of approximately 75 μm . Further details of the beamline optics and data acquisition methods have been published elsewhere.¹

B. Experimental results

We have studied GaAs, GaSb, InSb, and InAs and find that upon pressure release, all these compound semiconductors transform back to the zinc-blende structure. A typical pressure cycle for InAs is shown in Fig. 2. In this figure, IP diffraction patterns of InAs are shown prior to the application of pressure, after the structural transition to the NaCl configuration, and again at ambient pressure after recovery. Both the untransformed zinc-blende and high-pressure NaCl structure diffraction pat-

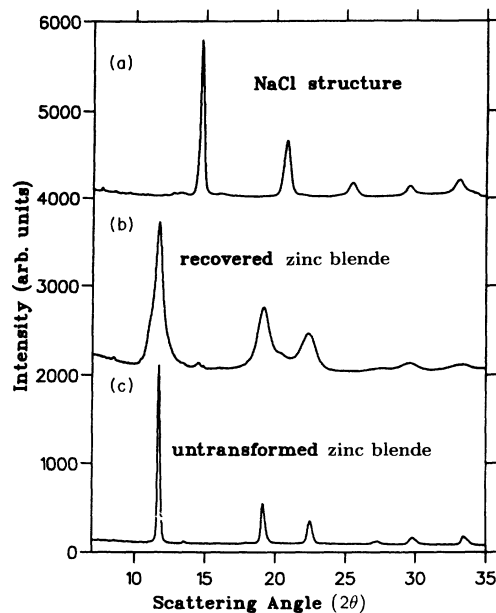


FIG. 2. High-sensitivity powder x-ray diffraction patterns of InAs (a) prior to the pressure-induced transition to the NaCl structure, (b) after recovery at ambient pressure, and (c) in the metallic NaCl structure. The broadened powder lines in (b) are indicative of a highly defected microstructure although the peak positions are clearly identifiable as being due to the zinc-blende phase. No unindexable lines are observed. The weak features observable in (b) at roughly 15° and 22° are identified as remnants of the NaCl phase. Such reversible transitions have also been found in GaAs, InSb, and GaSb with the recovered phase being characterized by extended defects in all cases.

terns are characterized by very sharp powder lines. Upon depressurization, the diffraction pattern of the recovered form is found to be characterized by extremely broad powder diffraction peaks suggestive of a highly defected microstructure. The structure of the recovered form is, however, clearly identified as zinc blende. Despite the extreme sensitivity of the IP detector, no other crystalline phase of InAs was observable at any point during depressurization from the metallic modification. Similar IP diffraction sequences have been recorded for the other III-V semiconductors mentioned above. Also, our previous experimental and computational studies suggest that the microstructure of recovered III-V compound semiconductors is characterized (over length scales of several tens of angstroms) by short-range order of the atomic species over the lattice sites.

A study by Besson *et al.*¹⁶ has recently been performed which focused in detail on the forward and reverse transitions between the zinc-blende and the high-pressure phase (phase II) of GaAs. Comparison of the observed diffraction line positions of recovered GaAs with those of untransformed GaAs showed very close agreement. Despite the reversibility of the pressure-induced transition in GaAs, a substantial degree of hysteresis was revealed in extended x-ray-absorption fine-structure mea-

measurements which showed that a 16 GPa pressure interval existed between completion of the forward and reverse transitions.¹⁶ These authors also applied other techniques in order to better determine the pressure range in which the thermodynamic transition point of GaAs must lie. The first evidence of transition on the upstroke was recorded at 13.5 GPa by optical transmittancy measurements and the first indication of retransformation to fourfold coordinated material on the downstroke was observed by Raman scattering at 10.5 GPa. Therefore the difference in pressure between that at which the transition from fourfold to sixfold coordination is first observed on the upstroke and that at which the reverse transition is observed is 3.0 GPa. This pressure difference gives some indication of the ease of transition between the two phases where a relatively large value of the difference suggests a relatively difficult transition route.

We have performed high-sensitivity IP experiments on silicon with a view to determining the pressure at which the metallic phase first begins to transform to BC8. This will allow an estimate to be made of the fourfold-sixfold pressure hysteresis and therefore an estimate of the relative ease of transition between the two phases to be deduced.

The silicon sample of the present study was initially pressurized to 12.4 GPa. The pressure relaxed to 11.2 GPa as the transition to the metallic phase proceeded. The diffraction pattern collected at a pressure of 11.2 GPa is shown in Fig. 3(a). Upon gradual pressure reduction to 10.6 GPa, a small amount of the BC8 phase was observable. The IP diffraction pattern recorded at this pressure is shown in Fig. 3(b). At this pressure, it was found that a small distortion of the BC8 (Si-III) structure away from cubic symmetry occurs and that this distortion gradually diminishes as pressure is further reduced. We refer to this structure as *d*-BC8.¹⁷ The difference in pressure between sixfold formation upon pressure increase and BC8 formation upon downloading is therefore between 0.6 and 1.8 GPa for silicon. It should be emphasized that this value is greater than that which would be obtained from short-range probes as it has been determined entirely from diffraction measurements. This is because long-range crystalline order of each phase must be established in the sample before it can be detected experimentally by diffraction-based techniques. Thus the relatively small value for the pressure difference is in marked contrast to that found for GaAs. This suggests that a relatively easy transition route from the sixfold coordinated metallic phase to BC8 exists in silicon but that GaAs follows a more difficult route back to zinc-blende without transiting the SC16 structure.

It therefore appears that, while pressure-induced structural transitions in group-IV semiconductors are irreversible, they are reversible (with hysteresis) in the compound III-V semiconductors and under no circumstances have the diatomic equivalents of the BC8 structures been observed. A general summary of the existing experimental results on pressure-induced polymorphism in group-IV and III-V semiconductors is illustrated by the sketch shown in Fig. 4. To our knowledge, InP is the only III-V compound which experiment has revealed may ex-

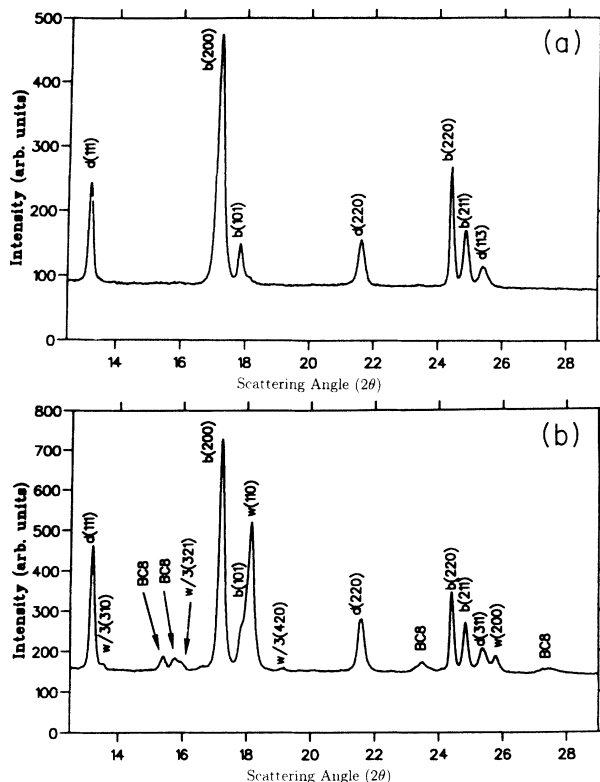


FIG. 3. (a) X-ray powder diffraction pattern of silicon at 11.2 GPa. Data have been collected using an IP area detector. The sample has partially transformed to the β -Sn structure at this pressure and the diamond component is used as the pressure calibrant. $d(hkl)$ and $b(hkl)$ denote peaks from the diamond and β -Sn structures, respectively. (b) Image plate x-ray powder diffraction pattern of the same silicon sample at 10.6 GPa after depressurization from 11.2 GPa. Three phases of silicon are present: $d(hkl)$ denotes peaks from the diamond structure, $b(hkl)$ denotes those from the β -Sn phase, and BC8 denote those of the *d*-BC8 phase (see the text). The $W(hkl)$ and $W/3(hkl)$ identify tungsten gasket lines due to diffraction from the principal monochromatic synchrotron beam and its third harmonic.

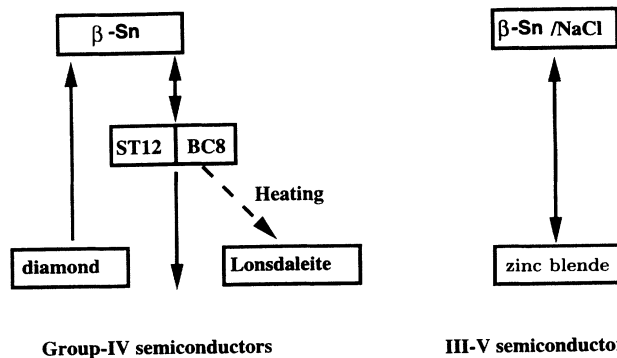


FIG. 4. Schematic diagram summarizing the existing experimental results on pressure-induced structural transitions in group-IV and III-V semiconductors. Up and down arrows represent pressure increase and decrease, respectively. All results are for room temperature measurements except for the high-temperature BC8 to lonsdaleite transition represented by a dotted arrow in the figure.

hibit an irreversible pressure-induced structural transition. Menoni and Spain have performed angle dispersive powder diffraction using a position-sensitive detector¹⁸ and have reported that InP-II (NaCl structure and metallic) transformed, upon depressurization, to a structure which was distinct from zinc blende. However, no further interpretation of the diffraction pattern was given. Recent IP experiments at SRS have failed to reproduce these findings.¹⁹

IV. COMPUTATIONAL METHOD

We apply the density functional theory with pseudopotentials and the local density approximation to exchange and correlation.^{20–22} Nonlocal ionic pseudopotentials generated by the Kerker method²³ are used to represent the electron-ion interaction. Kleinman-Bylander separation of the nonlocal parts is also used.²⁴ Ionic positions are relaxed under the influence of Hellmann-Feynman forces until the calculated forces are below 0.04 eV/Å. A cutoff energy of 250 eV for the plane wave basis set is used and is sufficient to converge energy differences. We use two computer codes (CASTEP and CETEP), which we have developed for implementation of total-energy calculations on large systems. An iterative strategy using the conjugate gradients optimization method is used to relax the electronic configuration to its ground state for given ionic positions. Further details of these codes are given elsewhere.²⁵

We consider the semiconductors GaAs, InAs, and AlSb in the SC16 structure as these exhibit a wide variation in ionicity and bond length. The initial configuration for each of the compounds is based on that of BC8-silicon for which both free positional parameters x_1 and x_2 are set to 0.1003 in accordance with x-ray powder diffraction results. This value was optimized at each volume considered. Identical sets of four equally weighted special k points in the Brillouin zone²⁶ at which to sample the energy bands were chosen for each structure. We found that increasing the k -point set to the $6 \times 6 \times 6$ special k -point set gave no appreciable energy change for any of the three compounds considered here.

V. THEORETICAL RESULTS

A. Total-energy calculations and structural relaxation of SC16

The results of total-energy calculations on GaAs, InAs, and AlSb are shown in Figs. 5(a)–5(c). For GaAs, the optimum value for the lattice constant was found to be 6.750 Å with the value of the positional parameters x_1 and x_2 being $x_1 = 0.0947$ and $x_2 = 0.1034$, respectively. The two Ga-As bond lengths in the BC8 structure are 2.4325 Å and 2.3510 Å, which are, respectively, 0.6% and 3.9% shorter than the zinc-blende bond length of 2.4481 Å. For InAs, the optimal values for the positional parameters are $x_1 = 0.0988$ and $x_2 = 0.1037$.

The calculated volume dependence of the bond lengths

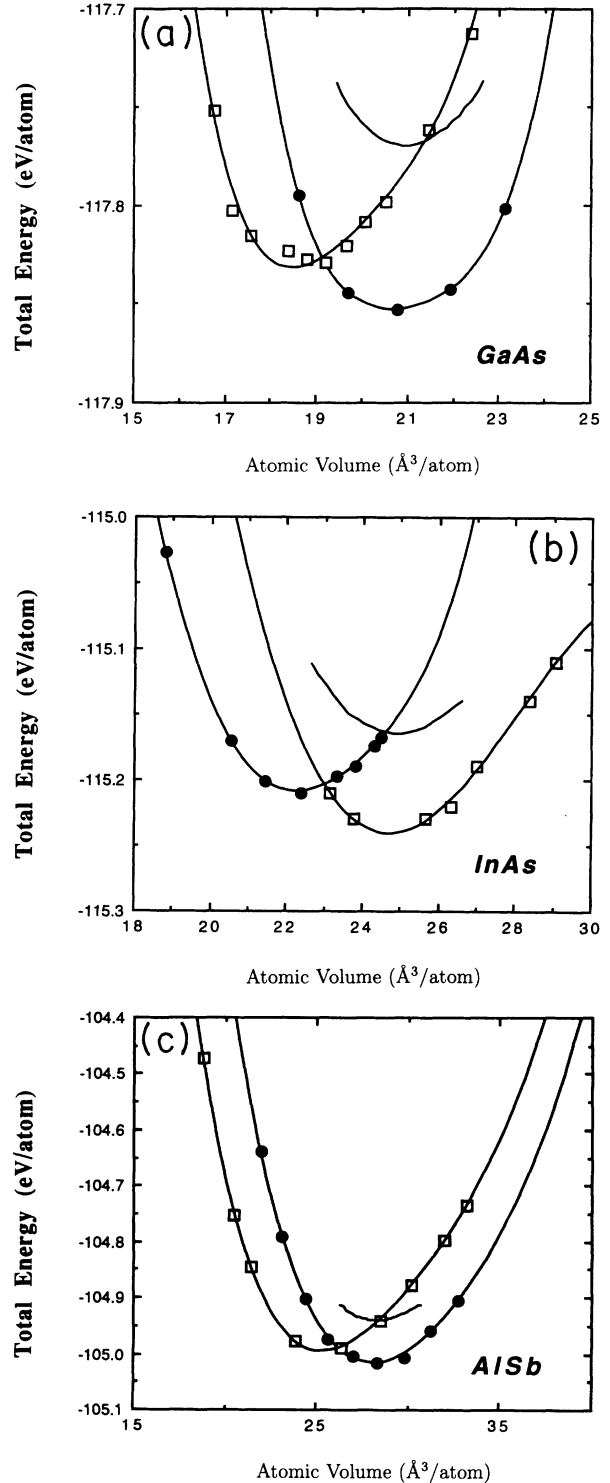


FIG. 5. The total energy of (a) GaAs, (b) InAs, and (c) AlSb, in the zinc-blende and SC16 structures. The energy differences, δE , between the SC16 and zinc-blende structures are 0.0275, 0.0293, and 0.022 eV/atom, for GaAs, InAs, and AlSb, respectively. Further structural details and transition pressures for the zinc blende to SC16 transition are shown in Table I. In (a)–(c), the zinc-blende phase is denoted by circles and the SC16 phase by squares. A polynomial fit to the data points is also shown. The energy vs volume under hydrostatic conditions for the wurtzite structure is shown by the solid curve.

is shown in Fig. 6 for GaAs and InAs. The calculated response for BC8-Si is also shown for comparison. It is found that the response to compression in BC8-Si and SC16 compounds is similar. As was found for BC8-Si,⁷ a crossover point exists at extreme compressions at which the *A* bond of the SC16 structure becomes longer than the *B* bonds for each of the compounds.

The total-energy differences between the BC8 and zinc-blende structure for these three materials are 0.0275 eV/atom for GaAs, 0.0293 eV/atom for InAs, and 0.0228 eV/atom for AlSb. These energy differences are much less than the 0.11 eV/atom difference (between the diamond and BC8 structures) reported for silicon.⁷ This reduction in the energy difference may be due to the fact that the partially ionic character of the III-V compounds favors the denser SC16 structure, while the fourfold coordination can simultaneously accommodate covalency.

Empirical pseudopotential and tight-binding calculations by Cohen and Joannopoulos¹² have revealed a clear energy gap in the electronic density of states of SC16-GaAs of the same magnitude as that found in the zinc blende and wurtzite structures. Furthermore, these authors have suggested that like-species bonds must be present in amorphous heteropolar semiconductors in order to account for the observed reduction in energy gap. The electronic band structure of BC8-Si has been investigated by Biswas *et al.*¹¹ It was reported that the valence and conduction bands are in contact at the Brillouin zone *H* point and that band overlap occurs between the valence band at *H* and the conduction band at the *F* point, suggesting that BC8-Si is semimetallic. In the present calculations, we have made the assumption that the SC16 compounds are semiconducting and have subsequently investigated the possibility that such structures might be semimetallic. Biswas *et al.* have also estimated that the error (in total energy) incurred in neglecting possible semimetallic properties¹¹ of BC8 silicon is less than 0.005 eV/atom and we consider our errors to be of a similar order of magnitude. In any case, inclusion of any refinements to the present calculations arising from semimetallic electronic structures would serve to reduce even further the energy differences between the SC16 and zinc-blende structures which we report above. Thus, consideration of energy differences between structures is not sufficient to account for the fact that SC16 structures have not been observed in high-pressure experiments. Next, we consider the calculated transition pressures.

For all compounds considered in this work, the calculated pressure at which the zinc-blende phase undergoes a pressure-induced structural transition to the SC16 configuration ($P_t^{\text{ZB} \rightarrow \text{SC16}}$) is significantly lower than the corresponding transition pressure associated with the semiconducting zinc blende to sixfold coordinated metal transition $P_t^{\text{ZB} \rightarrow \text{metal}}$. For example, GaAs is predicted in these calculations to transform from zinc blende to SC-16 at the modest pressure of 2.0 GPa whereas the earliest experimental indications of a structural transition are not observed until 16.4 GPa with the transition being to the sixfold coordinated GaAs-II structure.¹⁶ As stated previously, the reverse transition (back to zinc blende) was

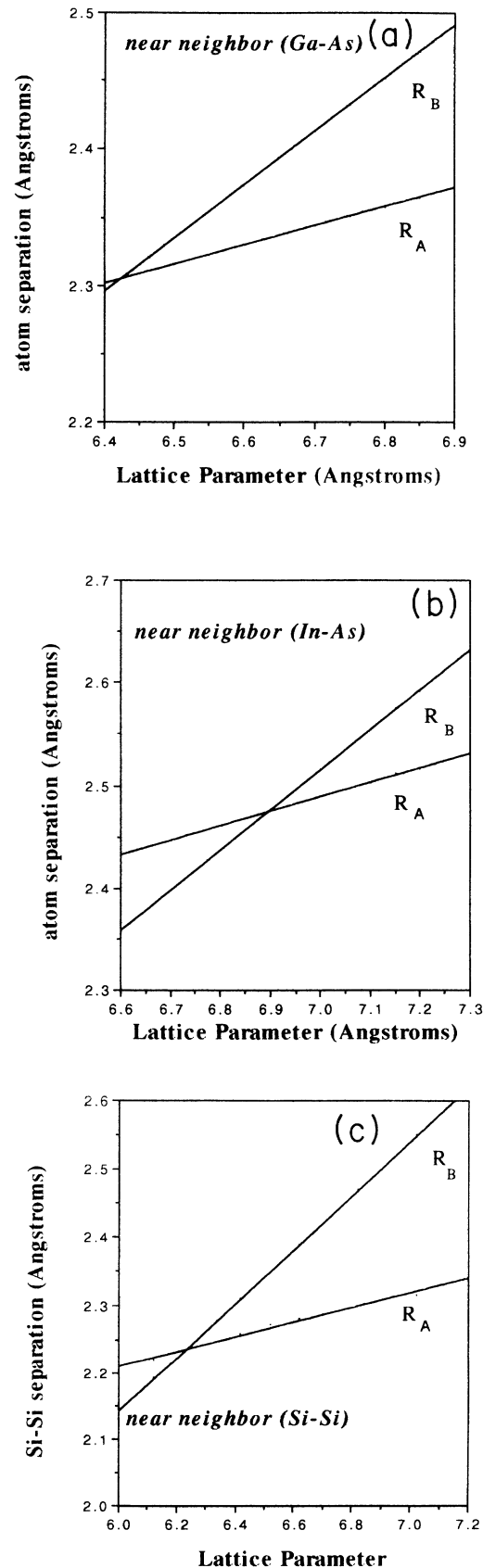


FIG. 6. Calculated variation of bond lengths with unit cell volume in the SC16 structures of (a) GaAs and (b) InAs. The behavior of silicon is shown for comparison in (c).

found not to be complete until 5.5 GPa.

On the basis of our total-energy calculations, we therefore conclude that the SC16 structure is a stable high-pressure modification of III-V semiconductors. Moreover, the results suggest that the first pressure-induced transition in the III-V compounds will be to the SC16 structure rather than to sixfold coordinated β -Sn or distortions thereof. In all three of these compounds we find that the SC 16 structure is approximately 10% denser than the zinc-blende structure. The results of these calculations are summarized in Table I.

It must be emphasized that our calculations yield only total-energy differences between structures at zero temperature and take no account of mechanical or kinetic factors associated with phase transitions. It is clear, however, that such factors must play an important role. In particular, structural transitions between topologically distinct covalent semiconductors (having highly directional covalent bonding) are likely to involve greater kinetic barriers than will transitions to metallic structures having far less directionality.

B. Electronic structure of SC16-GaAs

In Fig. 7 is shown the calculated electronic energy band structure. The density of occupied states exhibits a close resemblance to that reported from previous empirical pseudopotential calculations.¹² However, as is evident from inspection of the band structure, the valence and conduction bands touch at the Γ point of the Brillouin zone. In view of the well-known inadequacies of density functional theory in determining electronic excitation energies in solids, we are not in a position to investigate this issue further in the present paper. Partial reduction of the calculated energy gap may be due to the fact the two bond lengths in the fully relaxed structure of SC16-GaAs are both smaller than the ideal value. This situation would have the effect of broadening the p -like region (-4.0 – 0 eV) of the density of states.¹²

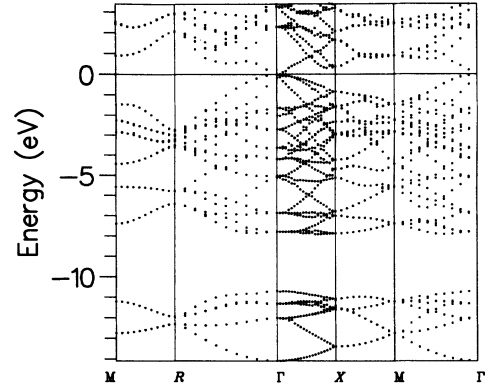


FIG. 7. Electronic energy band structure for the SC16 structure of GaAs. These density functional calculations predict that the valence and conduction bands are in contact at the Γ point of the Brillouin zone.

C. Valence charge density of III-V compounds in the SC16 structure

If the ionicity of the Ga-As bond were significantly higher in the SC16 structure than in the zinc-blende structure it could be argued that wrong-bond defects (which are likely to be present in the high-pressure and recovered phase²) would be more unfavorable in the SC16 structure than in either the zinc-blende or β -Sn phases. As discussed more fully in a later section, SC16 formation could conceivably be kinetically precluded if the wrong-bond energy were sufficiently high.

To explore this possibility, we have investigated the ionic character of the Ga-As bond in the zinc-blende and SC16 structures using the prescription given recently by Garcia and Cohen.²⁷ Their method allows an ionicity scale to be constructed from first principles using the overall asymmetry of the charge density as the fundamental quantity. According to this scheme, the charge density $\rho(\mathbf{r})$ is decomposed into symmetric and antisym-

TABLE I. Results of total energy pseudopotential calculations on several compound semiconductors in the SC16 structure (diatomic equivalent of BC8). Values for $P_t^{ZB\ metal}$ are taken from experimental results and represent upstroke measurements. Substantial hysteresis is known to exist, and downstroke measurements on GaAs reveal that the reverse transition to the zinc-blende structure is not complete until 5.5 GPa. The structural information given below is obtained from fits to the energy vs volume curves using the Murnaghan equation of state; units of energy are eV/atom, those of volume are $\text{\AA}^3/\text{atom}$, and the units of pressure are GPa.

Compound	$\delta E^{SC16\ ZB}$	V_0	x_1	x_2	$P_t^{ZB\ SC16}$	$P_t^{ZB\ metal}$
GaAs	0.0275	20.727	0.0947	0.1034	2.0	13.5 ^a
InAs	0.0293	22.501	0.0988	0.1037	1.7	7.0 ^b
AlSb	0.0228	25.439	0.1002	0.1059	1.4	8.6 ^c
Si	0.1100	17.480	0.1001	0.1001	11.0	10.3 ^d

^aReference 16.

^bReference 40.

^cReference 41.

^dReference 10.

metric parts. The origin of the coordinates is defined so that atoms of different species are interchanged upon inversion. The origin is therefore placed at the halfway point along the A bond. Implementation of the method involves the Fourier decomposition of the symmetric and antisymmetric parts of the charge density. One can derive a measure of the strength g of the symmetric and antisymmetric parts of ρ over the entire volume of the unit cell. We have applied this method to GaAs and find that the value of g for GaAs in the zinc-blende phase is 0.3014, which agrees well with the value of 0.316 reported by Garcia and Cohen.²⁷ The value for g in the SC16 structure is found to be 0.3090. This near equality of the calculated ionicities suggests that wrong-bond energies will be similar; however, the effect of atomic size should also be considered. This will be greater in the denser SC16 structure.

D. III-V compounds in the wurtzite structure

Under heat treatment, BC8 silicon transforms to the lonsdaleite structure. To examine whether the nonobservation of SC16 is due to immediate decomposition via wurtzite (the compound analogue of lonsdaleite), we have carried out calculations on the wurtzite phase of GaAs, InAs, and AlSb.

The wurtzite phase is characterized by two lattice parameters c and a and an internal parameter u . To compile a curve of energy against volume it is necessary to minimize the enthalpy at a range of pressures. An equivalent procedure is to minimize the energy as a function of c , a , and u . Due to the Pulay stresses arising when the basis set is changed, it is desirable to keep the unit cell unchanged during a relaxation of the electrons and the internal parameter. Consequently, we have followed the second scheme for constructing the E vs V curve.

For each material, we have calculated the energy at an optimized value of u for a series of c and a parameters around the minimum. Interpolation of this data has been used to produce the contour map (Fig. 8) of energy against volume and the c/a ratio. From these maps a hydrostatic line is constructed, being the c/a ratio which gives the minimum energy at a given volume. The energy-volume curves shown in Figs. 5(a)–5(c) are then projection of this line along the energy surface onto the volume axis.

For exact calculation of the c/a ratios, we concentrated on the region close to the minimum at the optimum volume. We found that the energy differences here were very small and the data were sensitive to the discreteness of the number of plane waves in the basis set, since the basis set is not complete and a finite k point set was used. The problem is due to the fact that as the unit cell volume changes, so do the number of basis states. This can be compensated for using the scheme of Francis and Payne,²⁸ which gives rise to smooth curves of energy against c/a from which c/a can be found.

The principle of the method is to derive a relationship between the calculated total energy $E_{\text{tot}}[c, N^{\text{PW}}(c, E_{\text{max}})]$ and the required energy

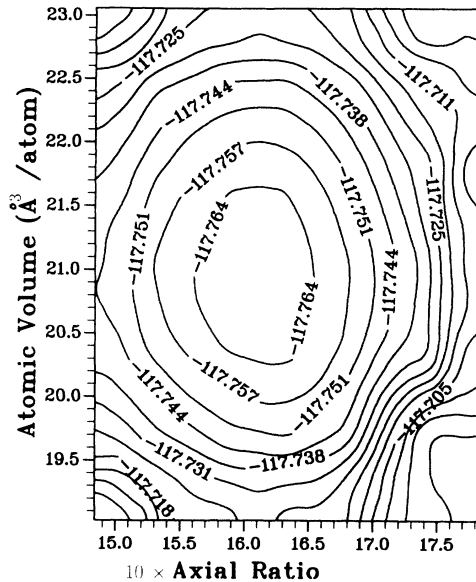


FIG. 8. A contour plot of corrected total energy as a function of atomic volume and the axial ratio (c/a) for wurtzite GaAs. From plots of this type, the energy vs volume relation under hydrostatic conditions can be constructed by projecting the line tracing the minimum energy at a given volume onto the volume axis. Such projections are shown in Figs. 5(a)–5(c).

$E_{\text{tot}}(c, E_{\text{max}})$ at some lattice parameter c , where N^{PW} is the number of plane waves in the basis and is itself a function of c and cutoff energy E_{max} . Francis and Payne consider differentials of the total energy and derive the following relationship:

$$E_{\text{tot}}(c, E_{\text{max}}) = E_{\text{tot}}[c, N^{\text{PW}}(c, E_{\text{max}})] - \frac{2E_{\text{max}}}{3} \frac{\partial E_{\text{tot}}(c, E_{\text{max}})}{\partial E_{\text{max}}} \times \ln \left(\frac{N^{\text{PW}}(c, E_{\text{max}})}{gc} \right), \quad (4)$$

where g is the continuum limit expression for the density of plane wave states as a function of E_{max} . Only at complete plane wave convergence of the total energy will the derivative with respect to E_{max} vanish. Away from this regime, the data must be “smoothed” by this correction if energy differences are small enough to be sensitive to the discrete changes in basis set.

An example of this smoothing (For AlSb) is shown in Fig. 9. Table II shows that in each case the equilib-

TABLE II. Minimum energy differences between the zinc-blende and wurtzite structures of GaAs, InAs, and AlSb in eV/atom. Also shown are the values for the optimal axial ratio and atomic volume. The wurtzite phase of the III-V compounds is found to be unstable at all pressures.

Compound	$\delta E^{\text{ZB wurtz}}$	c/a ratio	V_0
GaAs	0.084	1.614	21.0
InAs	0.078	1.609	25.0
AlSb	0.073	1.607	28.3

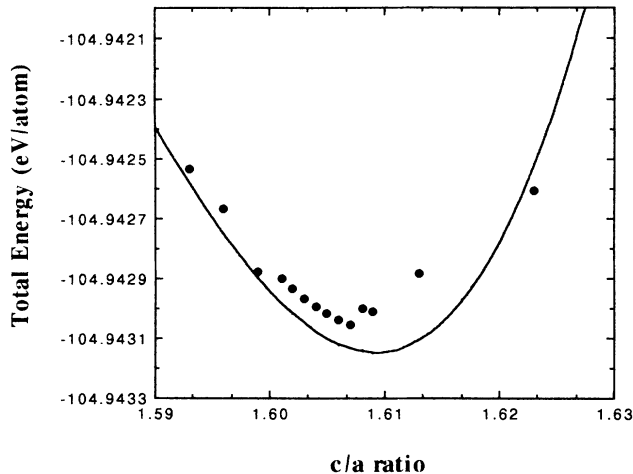


FIG. 9. The calculated total energy as a function of the c/a ratio for wurtzite AlSb (solid circles). These data have not been corrected for the fluctuations in the number of plane waves included in the basis set. The solid curve shows data which have been corrected according to the scheme proposed by Francis and Payne (Ref. 28).

rium volume was found to be slightly larger than that of zinc blende, with the binding energy being about 0.07 eV/atom higher. The wurtzite structures are therefore not stable at any pressure. In all cases the c/a ratio is slightly smaller than the “ideal” value of $\sqrt{8/3}$, as they are in stable wurtzite systems. This devalues the usefulness of the empirical rule that stable wurtzites have subideal c/a ratios.²⁹ A summary of the results of our calculations on wurtzite structures is shown in Table II. In previous pseudopotential studies on stable wurtzites both subideal [in AlN (Ref. 29)] and supraideal [in GaN (Ref. 30)] c/a ratios have been found.

E. *Ab initio* molecular dynamics studies and mechanical stability of SC16 GaAs

We have not yet explored mechanical stability which a true stable or metastable phase must possess. For a structure to be mechanically stable, positive restoring forces must oppose any small displacement of an atom about its equilibrium position. An equivalent statement is that phonon frequencies must be greater than zero (apart from Γ -point acoustic modes) throughout the Brillouin zone and for all polarizations.

Ideally, one should investigate all possible vibrational modes in order to fully explore the criterion for mechanical stability. To achieve this in an *ab initio* calculation, one would need to either apply the density functional molecular dynamics method to very large supercells or to implement a linear response scheme.³¹ As a result of the large unit cell of SC16, we will investigate only the stability of the zone center phonon modes in the present paper.

We apply the first-principles molecular dynamics method of Car and Parrinello³² which allows for fixed

temperature molecular dynamics in which forces acting on ions are calculated entirely from density functional theory. Periodic boundary conditions are used. A molecular dynamics step consists of relaxing the electrons to their ground state and then allowing the ions to move by integrating the equations of motion with a time step of 0.5 fs. The electronic wave functions have to be well converged between each step to ensure that the Hellmann-Feynman forces are correct—the error on the Hellmann-Feynman forces occurring from wave functions that are not fully converged are of first order in the wave functions. Therefore between each molecular dynamics step, the total energy was converged to better than 10^{-4} eV per ionic degree of freedom. This ensures that the system was kept close to the Born-Oppenheimer surface at all times.

The initial configuration was that of the fully relaxed structure where each atom is given a random velocity corresponding to an initial temperature of 300 K. The temperature was maintained close to this by use of a Nosé thermostat.³³ This “thermostat” introduces a coupling of the system to an external heat reservoir which has the effect of maintaining the average temperature of the ions at some fixed value. The unit cell dimensions were kept constant; therefore thermal expansion is not incorporated into the simulation, although such effects are expected to be small.

The mechanical stability of the structure can be examined by extracting the vibrational modes. In this case a single unit cell of the SC16 structure is considered; therefore, the allowed phonons are the nonzero Γ -point modes. These can be calculated from the velocity autocorrelation function

$$A(t) = \frac{\langle \mathbf{v}(0) \cdot \mathbf{v}(t) \rangle}{\langle \mathbf{v}(0) \cdot \mathbf{v}(0) \rangle}, \quad (5)$$

where $\mathbf{v}(t)$ is the ionic velocity and the angular brackets denote the ensemble average. This is shown in Fig. 10(a). It can be seen that $A(t)$ oscillates about zero indicating that the (Γ -point) vibrations are stable.

The spectral density (phonon density of states at the Γ point) was then obtained by Fourier transforming the velocity autocorrelation function. The result is shown in Fig. 10(b).

The effect of disorder on the vibrational spectrum of III-V semiconductors is expected to be similar to its effect on the electronic spectrum. That is, to a first approximation, disorder introduces broadening relative to the crystalline density of states. In our calculation of the Γ -point density of states, we find that the positions of the prominent features (at approximately 2 and 8 THz) correspond to the positions of the TA and TO phonon branches of the zinc-blende phase.³⁴

This application of first-principles molecular dynamics to compound semiconductors in complex crystalline phases appears to be a promising method of investigating the effects of disorder on certain aspects of vibrational spectra. In this respect it would be particularly interesting to study compound versions of the ST12 structure in order to probe the effects of like-species bonding on

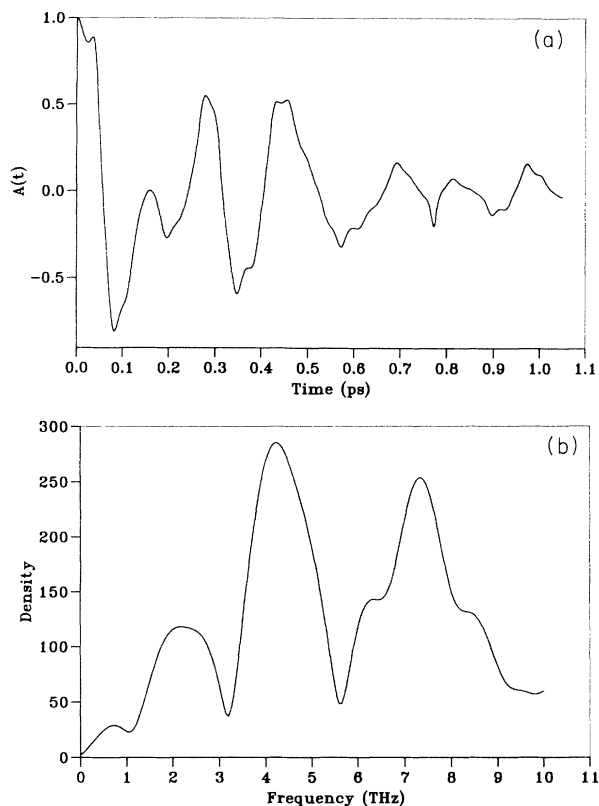


FIG. 10. Velocity autocorrelation function for (a) SC16 GaAs as determined from density functional molecular dynamics and (b) its spectral density corresponding to the nonzero frequency Γ -point phonon modes.

the vibrational properties. This will be the subject of a future paper.

The vibrational density of states obtained for SC16 GaAs in this way is similar to that of BC8 silicon.³⁵ Thus the nonexistence of SC16 cannot be attributed to entropic effects.

F. Geometric considerations of transition kinetics

We have attempted to deduce a plausible transformation mechanism for the metallic to BC8 transformation in silicon and attempted to determine whether this will be applicable to the compounds.³⁶ To do this we have started with the Imma structure³⁷ for silicon reported recently by Nemes *et al.*¹⁰ This is a distortion of the β -Sn structure and is the monatomic analogue of the high-pressure Imm2 phase found in several III-V compounds. From this structure we have determined the eight nearest neighbors, and constructed an eightfold coordinated graph. For the BC8 structure, we have constructed a similar graph where the connectivity is defined by the five nearest neighbors. Using a computer, we have searched all the possible mappings of atoms from one graph to the other to find the one which preserves the largest number of bonds. We have found a unique solution for which four out of five BC8 bonds are retained from the eightfold Imma configuration.

This topological argument does not tell us anything about the atomic motion in the transition. We can, however, attempt to relate the initial and final unit cells. In Fig. 11(a) we consider a cell containing four conventional Imma unit cells. The Imma structure used has $c/a = 0.538$, $b/a = 0.950$, a unit cell volume of 12.9 ($\text{\AA}^3/\text{atom}$), and the free positional parameter is 0.193. Concerted motion of chains involving half the atoms, together with shears of the lattice parameters, transforms the atoms in such a way that the fivefold BC8 structure is recovered with the minimum bond breaking as suggested by the topological graph transformation.

As this mechanism can be visualized as a coordinated motion of a chain of atoms, we refer to it as a “chain” mechanism, although it must be stressed that it is not a simple replacement sequence. In contrast we refer to the zinc blende $\rightarrow \beta$ -Sn transition observed in compounds as a “dislocation” mechanism, on the assumption that the inversion domain boundaries are formed by motion of partial superdislocations.²

It is clear from Fig. 11(b) that if we start with the ordered compound analogue of Imma, some of the bonds defined in the eightfold graph are between atoms of the same species. These bonds persist throughout the transformation and are still present in the final BC8 structure (see Figs. 12 and 13). Thus this mechanism would not

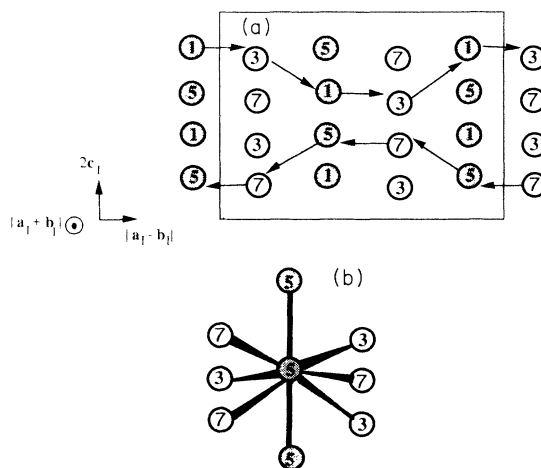


FIG. 11. (a) Projection diagram of an Imma unit cell, from the data for silicon of Ref. 10. This cell is four times the size of the conventional one (16 atoms), in the orientation from which it can transform to the standard BC8 cell shown in Fig. 12. The arrows depict the atomic motions required to effect the transformation: there are no movements perpendicular to the plane. Concordant with these atomic motions, the cell parameters transform to be cubic. The third axis of this cell comes out of the paper at an angle of 87° to the $|\mathbf{a} - \mathbf{b}|$ axis and at 90° to the c axis. Fractional elevations (in eighths) are shown as numbers inside the circles. The shadings indicate the atomic species in the ordered Imm2 compound equivalent structure. (b) illustrates the eight nearest neighbor connections in the Imma structure which were used in the computer search of mappings onto the BC8 graph (see the text and Fig. 12). The atom at elevation level 5 is chosen arbitrarily.

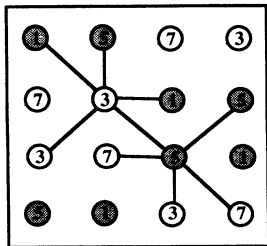


FIG. 12. The BC8 structure graph used in the computer search, showing the five nearest neighbors of two of the atoms. The elevations are the same as those shown in Fig. 11.

correctly transform the compounds to the SC16 structure with $P2_13$ symmetry. Moreover, the chain mechanism in silicon could be enhanced by vacancy migration along the chain, such that the atoms need move singly rather than in concert. This would not be possible in the compound analogues due to the different charge states of the vacancies. For these reasons we believe that while the chain mechanism may provide an easy transformation path in silicon, it is considerably more difficult in the compounds.

The dislocation mechanism would also be easier in the elements than in the compounds, though here the stress concentration in the dislocation core is great enough to form like-species bonds. Thus the kinetic barriers E to the various transformation mechanisms can be ordered as follows:

$$E_{\text{chain}}^{\text{elements}} < E_{\text{dislocation}}^{\text{elements}} < E_{\text{dislocation}}^{\text{compounds}} < E_{\text{chain}}^{\text{compounds}} \quad (6)$$

There is no direct evidence for any of these mechanisms; however, indirect evidence can be gleaned from the microstructure of the postrecovered phases. In silicon the negligible strain and fast kinetics of the transformation to BC8 is consistent with a fast diffusional transition such as the chain mechanism. By contrast, the highly deformed microstructure observed in InSb suggests a more tortuous path, with large strains required to force the

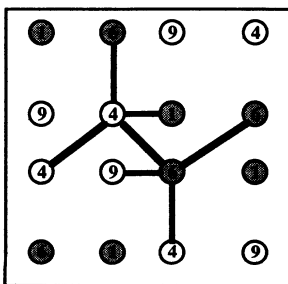


FIG. 13. The final BC8 structure with the fourfold bonds drawn in for two of the atoms. The square is the unit cell, the numbers being height in multiples of $\frac{1}{10}$ of the unit cell. Shading indicates the species type that would result if a diatomic phase transformed by the atomic movements shown in Fig. 11. Note the difference between this figure and Fig. 1.

normally sessile dislocations through the crystal, creating like-species bonds and leaving inversion domain boundaries, twins, etc. in their wake.

All routes between β -Sn and SC16 that do not result in like-species bonds in the final SC16 phase require very extensive bond breaking and intermediate wrong bonds. This would probably involve high energy barriers. It therefore appears that the III-V compounds do not form SC16 due to the easy transition path available for Si being precluded by the formation of at least one like-species bond per atom.

VI. CONCLUSIONS

We have shown that the results of *ab initio* pseudopotential calculations on the SC16 structure are at variance with experimental observations. Since these calculations are normally reliable and the predicted region of stability is large compared with possible sources of error in the calculation, this contradiction merits further attention.

The calculated transition pressures are around 1.5 GPa, almost an order of magnitude less than the pressure at which the zinc blende \rightarrow β -Sn transition is observed. This suggests that the SC16 phase is thermodynamically stable over a large range of pressures for all the III-V compounds considered here. This is in contrast to silicon, where, although the BC8 phase has been synthesized, pseudopotential calculations show that it is only metastable. It is similar to that of germanium where the intermediate phase is ST12.

The dichotomy of the existence of metastable BC8 and the nonexistence of stable SC16 can be resolved by considering the transformation kinetics. It is already known that the diamond \rightarrow BC8 transition does not occur directly in Si or Ge within a reasonable timespan. Furthermore, the retransition BC8 \rightarrow diamond has not been observed: even at elevated temperatures BC8 silicon only transforms to the lonsdaleite (hexagonal diamond) structure. The wurtzite phase of III-V compounds has higher energy than SC16. While an analogy with silicon suggests that it may be easier for SC16 to decompose into wurtzite than directly to zinc blende, we find that this transition is thermodynamically impossible.

For the SC16 structures, it is likely that the transformation kinetics will be even slower than in monatomic BC8. The zinc-blende semiconductors have very slow diffusion and, unlike silicon, remain brittle up to the melting point. This is due to the partly ionic nature of the bonding which makes bonds between atoms of the same species unfavorable, an effect which is absent in diamond.

We have proposed a model for the β -Sn \rightarrow BC8 transition based on topological considerations of bond breaking. The picture of silicon as covalently bonded in these phases receives support from inspection of the valence charge densities^{7,38} and from the success of empirically based covalent models in describing these phases.^{35,39} The transition path that involves fewest broken bonds in BC8 does not correctly transform diatomic Imma to SC16—wrong bonds are created.

The proposed Imma to diamond pathway proceeds by dislocation motion in which the local stresses associated

with the dislocation are sufficiently strong to create a few wrong bonds in the compound analogue. The Imma to BC8 transition proceeds by coordinated motion of atoms. In silicon this process could be enhanced by vacancy migration. This does not introduce large local strains and is therefore blocked by the requirement of forming many wrong bonds in the compounds. Although both of these routes are speculative, they are consistent with the differing observed microstructures of the postrecovered phases.

Thus we conclude that the transformation between BC8 and SC16 and diamond and zinc blende will be slower in the compounds than in the elements. Since the transition has not been observed in either direction in any element, it is not surprising that we have not found it in the compounds. In contrast, the β -Sn \rightarrow BC8 transition is relatively easy in the elements (compared with β -Sn \rightarrow diamond). We have presented one possible route for this transition which requires few broken bonds and should therefore have a small kinetic barrier. However, this route does not transform the compounds correctly into SC16, so the possibility of creating SC16 due to favorable kinetics on depressurization is lost. Since SC16 is a thermodynamically stable phase, our results suggest that it would be formed by slow cooling from a melt at intermediate pressure. It is possible that it could also be formed by heating the metallic phase of the compound at pressures slightly above that of the diamond transition, but we are unable to estimate the kinetics of this

transition. Once formed, the large kinetic barriers would ensure that SC16 would be very long lived at ambient pressure.

Note added in proof: Since the writing of this paper, we have been made aware of the results of very recent high-pressure powder neutron diffraction experiments performed by S. Hull and D. Keen [Phys. Rev. B (to be published)]. These authors have identified the SC16 structure as a stable high-pressure modification of the I-VII semiconductors CuCl and CuBr. In view of this finding, it now appears that the relative energetics of structure adoption in group-IV, III-V, and I-VII semiconductors may be much more similar than they once appeared to be. Calculations of structural stability in copper halides are now underway. We are grateful to S. Hull and D. Keen for making their results available to us prior to publication.

ACKNOWLEDGMENTS

G.J.A. and J.C. acknowledge support from the Royal Society of Edinburgh. P.D.H. acknowledges support from the Leverhulme Trust. S.J.C. thanks the Science and Engineering Research Council for support. We are also grateful to Digital Equipment Corp. for loan of an Alpha-AXP supercomputer on which the calculations were performed and to D.W. Greig for assistance with graphics.

¹R.J. Nelmes, P.D. Hatton, M.I. McMahon, R.O. Piltz, J. Crain, R.J. Cernik, and G. Bushnell-Wye, *Rev. Sci. Instrum.* **63**, 700 (1992).

²J. Crain, G.J. Ackland, R.O. Piltz, and P.D. Hatton, *Phys. Rev. Lett.* **70**, 814 (1993).

³There have been recent experimental developments using combined Laue and single crystal x-ray diffraction methods which have the potential to provide information regarding the relationship between structures involved in first order transitions. R.O. Piltz (unpublished).

⁴B. Weinstein and R. Zallen, in *Light Scattering in Solids IV*, edited by M. Cardona and G. Güntherodt, Topics in Applied Physics Vol. 54 (Springer-Verlag, Berlin, 1984).

⁵R.H. Wentorf and J.S. Kasper, *Science* **338**, 139 (1964).

⁶J.S. Kasper and S.M. Richards, *Acta Cryst.* **17**, 752 (1964).

⁷J. Crain, S.J. Clark, G.J. Ackland, M.C. Payne, V. Milman, P.D. Hatton, and B. Reid, *Phys. Rev. B* **49**, 5329 (1994).

⁸M.T. Yin and M.L. Cohen, *Phys. Rev. Lett.* **50**, 2006 (1983).

⁹A. Mujica and R.J. Needs, *Phys. Rev. B* **48**, 17 010 (1993).

¹⁰R.J. Nelmes, M.I. McMahon, N.G. Wright, D.R. Allan, and J.S. Loveday, *Phys. Rev. B* **48**, 9883 (1993).

¹¹R. Biswas, R.M. Martin, R.J. Needs, and O.H. Nielson, *Phys. Rev. B* **35**, 9559 (1987).

¹²J.D. Joannopoulos and M.L. Cohen, in *Solid State Phys.* **31**, 71 (1976); and *Phys. Rev. B* **10**, 1545 (1974).

¹³R.W.G. Wyckoff, *Crystal Structures*, 2nd ed. (Interscience, New York, 1963), p. 121.

¹⁴W.R.L. Lambrecht, C. Amador, and B. Segall, *Phys. Rev. Lett.* **68**, 1363 (1992).

¹⁵R.J. Nelmes, M.I. McMahon, P.D. Hatton, J. Crain, and R.O. Piltz, *Phys. Rev. B* **47**, 35, (1993).

¹⁶J.M. Besson, J.P. Itié, A. Polian, G. Weill, J.L. Mansot, and J. Gonzalez, *Phys. Rev. B* **44**, 4214 (1991).

¹⁷At 10 GPa, a small rhombohedral distortion ($\alpha = 92^\circ$) is observed. The difference in intensity of the powder diffraction peaks with respect to those of the undistorted structure suggests that the atoms have moved slightly from their symmetry positions. The crystallographic details of this phase will be discussed more fully in a future publication.

¹⁸C.S. Menoni and I.L. Spain, *Phys. Rev. B* **35**, 7520 (1987); C.S. Menoni, H.D. Hochheimer, and I.L. Spain, *ibid.* **33**, 5896 (1986). In the second of these papers, irreversibility of the InP photoluminescence signal was reported, but the cause could not be unambiguously attributed to the formation of a distinct crystalline phase upon pressure release. Hysteresis effects and/or scatter from phase transition-induced defects would also be consistent with their observations.

¹⁹N.G. Wright (private communication).

²⁰W. Kohn and L.J. Sham, *Phys. Rev.* **140**, 1133A (1965).

²¹J.P. Perdew and A. Zunger, *Phys. Rev. B* **23**, 5048 (1981).

²²D.M. Ceperley and B.J. Alder, *Phys. Rev. Lett.* **45**, 566 (1980).

²³G.P. Kerker, *J. Phys. C* **13**, L189 (1980).

²⁴L. Kleinman and D.M. Bylander, *Phys. Rev. Lett.* **48**, 1425 (1982).

²⁵M.C. Payne, M.P. Teter, D.C. Allan, T.A. Arias, and J.D. Joannopoulos, *Rev. Mod. Phys.* **64**, 1045 (1992).

²⁶H.J. Monkhorst and J.D. Pack, *Phys. Rev. B* **13**, 5188

- (1976).
- ²⁷A. Garcia and M.L. Cohen, *Phys. Rev. B* **47**, 4251 (1993).
- ²⁸G.P. Francis and M.C. Payne, *J. Phys. C* **2**, 4395 (1990).
- ²⁹P.E. van Camp, V.E. van Doren, and J.T. Devreese, *Phys. Rev. B* **44**, 9056 (1991).
- ³⁰P.E. van Camp, V.E. van Doren, and J.T. Devreese, *Solid State Commun.* **81**, 23 (1992).
- ³¹T.W. Barbee, *Phys. Rev. B* **48**, 9327 (1993).
- ³²R. Car and M.Parrinello, *Phys. Rev. Lett.* **55**, 2471 (1985).
- ³³S. Nosé, *J. Chem. Phys.* **81**, 511 (1984).
- ³⁴M.H. Brodsky, *Topics Appl. Phys.* **8**, 228 (1975).
- ³⁵S.J. Clark, G.J. Ackland, and J. Crain, *Phys. Rev. B* **49**, 5341 (1994).
- ³⁶R.O. Piltz (unpublished).
- ³⁷The Imma structure is a known high-pressure phase of Si which is closely related to that of the β -Sn structure. See M.I. McMahon and R.J. Nelmes, *Phys. Rev. B* **47**, 8337 (1993) for a fuller discussion of the crystallography.
- ³⁸M.T. Yin and M.L. Cohen, *Phys. Rev. B* **26**, 5668 (1982).
- ³⁹G.J. Ackland, *Phys. Rev. B* **40**, 10351 (1989).
- ⁴⁰Y.K. Vohra, S.T. Weir, and A.L. Ruoff, *Phys. Rev. B* **31**, 7344 (1985).
- ⁴¹S.C. Yu, I.L. Spain, and E.F. Skelton, *Solid State Commun.* **25**, 49 (1978).

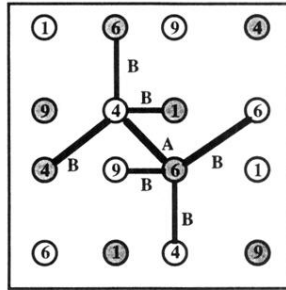


FIG. 1. Projection of the diatomic equivalent of the BC8 structure (SC16 structure) with $x_1 = x_2 = 0.1$. A cubic unit cell containing 16 atoms is shown and the bonds of the central tetrahedral unit are illustrated as black lines. No like-species bonds are present. Elevations in fractional units of $c/10$ are indicated by the numbers inside the circles. Different species are denoted by different shading.

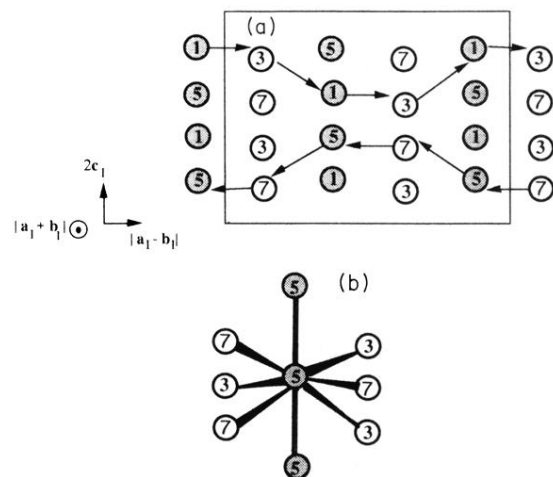


FIG. 11. (a) Projection diagram of an Imma unit cell, from the data for silicon of Ref. 10. This cell is four times the size of the conventional one (16 atoms), in the orientation from which it can transform to the standard BC8 cell shown in Fig. 12. The arrows depict the atomic motions required to effect the transformation: there are no movements perpendicular to the plane. Concordant with these atomic motions, the cell parameters transform to be cubic. The third axis of this cell comes out of the paper at an angle of 87° to the $|a - b|$ axis and at 90° to the c axis. Fractional elevations (in eighths) are shown as numbers inside the circles. The shadings indicate the atomic species in the ordered Imm2 compound equivalent structure. (b) illustrates the eight nearest neighbor connections in the Imma structure which were used in the computer search of mappings onto the BC8 graph (see the text and Fig. 12). The atom at elevation level 5 is chosen arbitrarily.

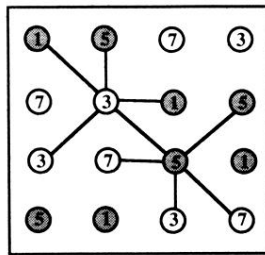


FIG. 12. The BC8 structure graph used in the computer search, showing the five nearest neighbors of two of the atoms. The elevations are the same as those shown in Fig. 11.

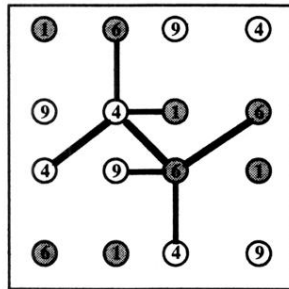


FIG. 13. The final BC8 structure with the fourfold bonds drawn in for two of the atoms. The square is the unit cell, the numbers being height in multiples of $\frac{1}{10}$ of the unit cell. Shading indicates the species type that would result if a diatomic phase transformed by the atomic movements shown in Fig. 11. Note the difference between this figure and Fig. 1.